sciendo

Reports on Geodesy and Geoinformatics, 2024, Vol. 118, pp. 127–135

DOI: 10.2478/rgg-2024-0021
Received: 3 September 2024 / Accepted: 25 November 2024
Published online: 20 December 2024

ORIGINAL ARTICLE

Implementation of the dual quaternion algorithm for 3D similarity-based coordinate transformation between Ghana's local geodetic datum and WGS84

Yao Yevenyo Ziggah [1*], Saviour Mantey [1] and Prosper Basommi Laari [2]

[1]Department of Geomatic Engineering, Faculty of Geosciences and Environmental Studies, University of Mines and Technology, P.O.Box 237, 00233, Tarkwa, Ghana
[2]Department of Environment and Resource Studies, Simon Diedong Dombo University of Business and Integrated Studies, P. O. Box WA64, 00233, Bamahu, Wa, Ghana

*yyziggah@umat.edu.gh

Abstract

Modern surveying practice has embraced the use of Global Navigation Satellite System (GNSS) technology due to its attainable precision and uncomplicated functionality. The adoption of this technology has therefore necessitated the transformation of coordinates between satellite-based and classical geodetic reference datums. It is known that the 3D similarity-based transformation models are the most widely used in the literature. However, one major limitation of such models is the representation of point rotations in space using Euler angles connected to X, Y, and Z-axes, which often leads to matrix singularities. To overcome this mathematical inconvenience, the dual quaternion is proposed. This paper implements the dual quaternion algorithm to transform coordinates between the World Geodetic System 1984 (WGS84) and Ghana War Office 1926. To perform the transformation, 31 common points were divided into two parts: reference and check points. The reference points, consisting of 24 common points that are evenly distributed across Ghana, were used to derive the transformation parameters. The remaining 7 points were used to evaluate the derived transformation parameters. The results confirmed that the coordinates transformed by the dual quaternion algorithm are in average agreement with the measured coordinates, with precision and accuracy levels of about 0.580 m and 1.023 m. The obtained results follow the Bursa-Wolf model that is already used by the Ghana Survey and Mapping Division to perform 3D transformations. Hence, the results satisfy cadastral applications, geographic information works, reconnaissance, land information system works and small-scale topographic surveys in Ghana.

Key words: coordinate transformation, dual quaternions, Global Navigation Satellite System, Bursa-Wolf model

1 Introduction

Performing three-dimensional (3D) coordinate transformations involves the use of translation, rotation, and scale parameters that unify and connect a non-geocentric system to a geocentric system and vice versa. Such a practice requires the use of 3D transformation models and their associated transformation parameters, which are determined using the traditional least squares approach. Although a plethora of transformation models are available in the literature, 3D similarity-based models such as Helmert, Bursa-Wolf, Molodensky-Badekas, and Veis are the most widely used and adopted for coordinate transformation by governmental mapping agencies, private sector, and field practitioners (Kheloufi and Dehni, 2023; Prasad and Prasanna, 2022; Hussain, 2022; Kalu et al., 2022; Ruffhead, 2021; Ansari et al., 2017, 2019; Elshambaky et al., 2018; Okiemute et al., 2018; Mihajlović and Cvijetinović, 2017; Doukas et al., 2017; Soler et al., 2016). The reason for wider application can be attributed to the attainable precision and uncomplicated functionality.

However, scholars (Zeng et al., 2018, 2019, 2020, 2022a,b, 2024;

Uygur et al., 2022; Bektas, 2022, 2024; Ioannidou and Pantazis, 2020, 2022; Shen et al., 2006) identify some mathematical inconveniences of the similarity-based models. One major limitation is the use of the Euler angle to represent the rotation between the reference axes of the geocentric and non-geocentric systems. Thus, Euler angle representation in trigonometric functions of sine and cosine can lead to dual solutions. In cases where the reference axes angles are smaller, there is a rapid change in the sine function. Besides, Euler angles exhibit interdependency between the reference axes when the rotational angle is $\pm 90°$ about the Y-axis (Bektas, 2022, 2024). Since the Euler angles lack mathematical attractiveness, the rotation, translation, and scale parameters are estimated in dual quaternions to overcome those enumerated challenges. The introduction of the quaternion eliminates the issue of matrix singularities. Table 1 gives a summary of recent quaternion-based coordinate transformation studies. These previous studies (Table 1) do conclude that all the variants of quaternion methods offer the mathematical attractiveness of less computational power, faster convergence, numerical stability, and no initial boundary conditions to implement the algorithm.

A comprehensive overview of the literature (Zeng et al., 2018, 2019, 2020, 2022a,b, 2024; Uygur et al., 2022; Bektas, 2022, 2024; Ioannidou and Pantazis, 2020; Shen et al., 2006) indicates that geographically, the quaternion and dual quaternion were applied and tested in geodetic reference systems found within the Western continents (e.g., Europe, Asia, etc.). No such studies exist in Sub-Saharan Africa where the national mapping reference systems are mostly dominated by non-geocentric datums. In general, the quaternion and dual quaternion methods are yet to be embraced wholeheartedly within Sub-Saharan Africa. Hence, there is the need to apply, test, and evaluate for the first time the capability of the dual quaternion algorithm to unify a highly heterogeneous classical geodetic system and satellite-based system in Sub-Saharan Africa (due to its establishment). This study selected and applied the dual quaternion approach over the quaternion. Unlike the quaternion, which considers only the rotation, the dual quaternion creates the opportunity to represent both the translation and rotation of the reference system (Ioannidou and Pantazis, 2022). It is important to mention that this study did not test other quaternion and dual quaternion algorithms because they were extensively investigated and compared in the literature (Zeng et al., 2018, 2019, 2020, 2022a,b, 2024; Uygur et al., 2022; Bektas, 2022, 2024; Ioannidou and Pantazis, 2020; Shen et al., 2006), where it was found that both methods produced identical coordinate transformation results. However, a significant difference lies in their computational procedures where they can be categorized as iterative (if initial approximation values for the unknown transformation parameters are needed) and noniterative.

Consequently, this study applied and tested the recently proposed non-iterative dual quaternion approach by Bektas (2022) in Ghana, a country located in the Western part of Africa where a non-geocentric datum called the Accra 1929 referenced on the War Office 1926 ellipsoid is used for its surveying and mapping activities. As is known from the literature, classical geodetic networks are highly heterogeneous due to the applied surveying methods and adjustment techniques, and employed personnel, among others (Varga et al., 2017; Poku-Gyamfi, 2009). Hence, it is an excellent opportunity to explore the computing performance of the dual quaternion algorithm for coordinate transformation from WGS84 to the War Office 1926 ellipsoid. To this end, the contribution of this study is to explore the practicality of dual quaternions as a convenient and reliable alternative 3D coordinate transformation technique in a classical geodetic datum located in a Sub-Saharan African country. This study will further raise awareness of the Surveying and Mapping Agencies in Africa necessary to grasp the potential and advantages offered by the dual quaternion approach for 3D coordinate transformation.

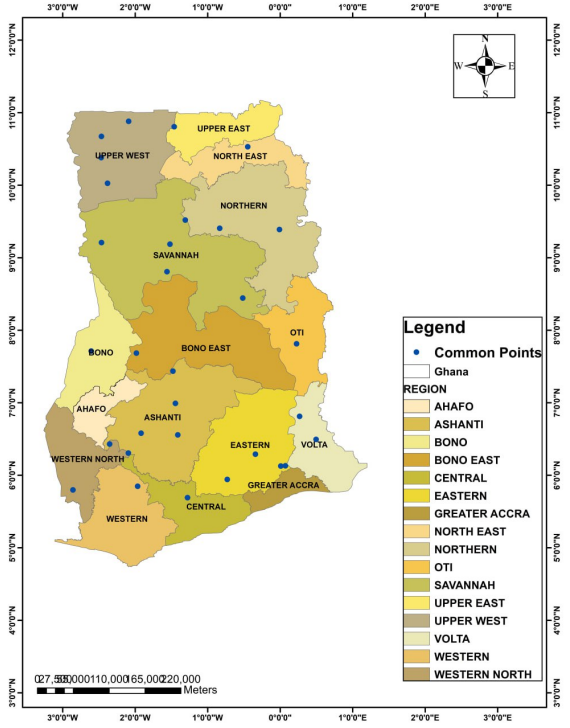

Figure 1. Distribution of common points across the regions in Ghana

2 Study area and data utilized

Ghana is the study area where this research was conducted. Located in West Africa, it lies between latitudes 4° 30' N and 11° N, and between longitudes 3° W and 1° E, covering a land area of 238,540 km^2. The Accra 1929 datum was officially established using the War Office 1926 as the reference ellipsoid. This non-geocentric system of reference is the official reference datum for surveying and mapping activities in Ghana. The War Office 1926 ellipsoid properties include a semi-major axis (6378299.99899832 m), semi-minor axis (6356751.68824042 m), and flattening (1/296). The grid coordinate system utilized in Ghana for cadastral and engineering applications is based on the Transverse Mercator projection. Globally, with modernization and advancement in technology, the geodetic fraternity adopted the use of Global Navigation Satellite System (GNSS) such as Global Positioning System (GPS) for surveying and mapping related works. The GPS is a geocentric system referenced to the World Geodetic System (WGS) 1984. Since Ghana's geodetic reference system is non-geocentric, there is a need to determine transformation parameters for the localization of the GPS-acquired data. To achieve that, this study applied a total of 31 common points distributed across the country for the coordinate transformation. The common points utilized are geodetic coordinates based on the War Office 1926 ellipsoid and WGS84. Figure 1 presents the distribution of the common points across 16 regions of Ghana.

3 Methods

3.1 Dual quaternion method applied

This study adopted the dual quaternion approach proposed by Bektas (2022). This approach was chosen and applied because of its simplicity in application, fast convergence rate, and unrequired use of initial approximate quaternion values for solution. The quaternion can be represented mathematically as:

$$q = (x_1 i + x_2 j + x_3 k) + w_0, \tag{1}$$

Table 1. Related work

Authors	Methods applied	Summary
Zeng et al. (2024)	Quaternion, dual quaternion, weighted total least squares	The study expressed the unit dual quaternion of the 3D similarity transformation in the form of errors-in-variables. The study revealed that the precision of the determined transformation parameters by the dual quaternion was better than the quaternion.
Zhao et al. (2024)	Generalized errors-in-variables (EIV), dual quaternion	The study identified the limitation of representing the rotation matrices using Euler angles and the impact of outliers on the parameters determined from distorted geodetic data. The EIV was proposed to solve the challenges, using dual quaternion to represent the rotations.
Bektas (2024)	Expanded dual quaternion algorithm, dual quaternion, Helmert 3D	The author proposed a novel dual quaternion algorithm that simultaneously transforms 3D coordinates and computes the related variance-covariance matrix of the transformation parameters.
Bektas (2022)	Dual quaternion, quaternion, Helmert 3D	The study pointed out that although Helmert 3D was the most widely used, it was limited because the rotational angles between reference systems were defined by Euler angles. The author concluded that no numerical superiority was observed between the dual quaternions and Helmert 3D. However, the dual quaternions exhibited faster convergence because the approach does not need initial starting values of the parameters to be determined.
Zeng et al. (2022a)	Orthonormal matrix algorithm, modified Procrustes algorithm, analytical dual quaternion algorithm	The results confirmed that all the methods employed were valid for performing point-wise transformations.
Ioannidou and Pantazis (2022)	Euler angles method, quaternion, dual quaternion	The results of the study revealed that the dual quaternion approach satisfactorily estimated the rotation parameters with the Euler angles, producing sizable variations. However, the study was inconclusive regarding the optimum way to estimate the translation and scale parameters.
Uygur et al. (2022)	Quaternion approach	The study presented how to apply the quaternion approach to retrieve Euler rotation angles in both symmetric and asymmetric 3D similarity transformations. The study went further to show how the covariance matrix could be retrieved for the derived transformation parameters. It was concluded that using the quaternion provided numerical stability and faster convergence to the solution.
Uygur et al. (2021)	Nine-parameter three-dimensional affine transformation model, quaternion approach	The study considered the (a)symmetric 3D nine-parameter affine transformation model using the quaternion-based approach to derive the transformation parameters and their associated covariance matrix. The effectiveness and consistency of the proposed approach were tested on five different case studies.
Ioannidou and Pantazis (2020)	Euler angles, quaternion, dual quaternion	This study investigated the reverse solution problem of the Helmert 3D transformation model by using Euler angles, quaternion, and dual quaternion algebra. The study concluded that the dual quaternion was better for estimating the rotation angles than the other methods investigated.
Zeng et al. (2018)	Unit dual quaternion, classical Procrustes algorithm, orthonormal matrix algorithm, Wang et al. (2014) approach	The study proposed an iterative solution and representation of the rotation and translation parameters of the Helmert 3D model using unit dual quaternion. The proposed approach can handle any rotation size. Comparable results were achieved with other methods considered.
Mercan et al. (2018)	Iterative solution for the Gauss-Helmert model, EIV, and quaternions	The study proposed an iterative solution for weighted symmetric 2D and 3D similarity transformation problems. The proposed algorithm does not need prior least squares estimation and can adequately handle issues regarding small rotation angles or small-scale factors between the source and the target datums.

where x_1, x_2, x_3 and w_0 are the numerical values. The i, j, and k are the imaginary components (basic quaternion units) that satisfy the following conditions (Kenwright, 2012; Zeng et al., 2024):

$$\begin{aligned} i^2 &= j^2 = k^2 = -1, \\ ij &= -ji = k, \\ jk &= kj = i, \\ ki &= ik = j, \\ ijk &= -1. \end{aligned} \tag{2}$$

In quaternions, the rotation matrix (R) can be evaluated using Equation (3):

$$R = \left(w_0^2 - q^T \times q\right) I_{3\times 3} + 2\left(q \times q^T\right) + w_0 \times C(q), \tag{3}$$

where $I_{3\times 3}$ is the unit matrix, $q = [x_1\, x_2\, x_3]^T$, and $C(q)$ is expressed in Equation (4):

$$C(q) = \begin{bmatrix} 0 & x_3 & -x_2 \\ -x_3 & 0 & x_1 \\ x_2 & -x_1 & 0 \end{bmatrix}. \tag{4}$$

Equation (5) establishes the relationship between R and the quaternions:

$$\begin{aligned} R &= \begin{bmatrix} \alpha_{11} & \alpha_{12} & \alpha_{13} \\ \alpha_{21} & \alpha_{22} & \alpha_{23} \\ \alpha_{31} & \alpha_{32} & \alpha_{33} \end{bmatrix} \\ &= \begin{bmatrix} w_0^2 + x_1^2 - x_2^2 - x_3^2 & 2(x_1x_2 + q_0q_3) & 2(x_1x_3 + w_0x_2) \\ 2(x_1x_2 + w_0x_3) & w_0^2 + x_1^2 + x_2^2 - x_3^2 & 2(x_2x_3 - w_0x_1) \\ 2(x_1x_3 - w_0x_2) & 2(x_2x_3 + w_0x_1) & w_0^2 - x_1^2 - x_2^2 + x_3^2 \end{bmatrix}, \end{aligned} \tag{5}$$

where:

$$\begin{aligned} w_0^2 &= \frac{1}{4}(1 + \alpha_{11} + \alpha_{22} + \alpha_{33}), \\ x_1^2 &= \frac{1}{4}(1 + \alpha_{11} - \alpha_{22} - \alpha_{33}), \\ x_2^2 &= \frac{1}{4}(1 - \alpha_{11} + \alpha_{22} - \alpha_{33}), \\ x_3^2 &= \frac{1}{4}(1 - \alpha_{11} - \alpha_{22} + \alpha_{33}). \end{aligned} \tag{6}$$

From the quaternions, the rotation angles can be expressed in Equation (7):

$$\begin{aligned} \varepsilon &= \operatorname{atan2}(-2(w_0x_1 + x_2x_3), (w_0^2 + x_1^2 - x_2^2 - x_3^2)), \\ \psi &= \operatorname{asin}(2(-w_0x_2 + x_3x_1)), \\ \omega &= \operatorname{atan2}(-2(w_0x_3 + x_2x_1), (w_0^2 + x_1^2 - x_2^2 - x_3^2)). \end{aligned} \tag{7}$$

As a representation for both translation and rotation parameters, the dual quaternion is utilized because the unit quaternion can only handle rotation. The dual quaternion is made up of eight elements or two quaternion elements (real and dual parts). In a single model, the dual quaternion can be expressed in compact form as shown in Equation (8):

$$q = q_r + q_d \times \mu, \tag{8}$$

where q_r and q_d are the real and dual parts of the quaternions with μ representing the additional dual number. To determine a new coordinate position, the dual quaternion defines the translation and rotation properties as follows:

$$\begin{aligned} q_r &= \alpha, \\ q_d &= t \times \alpha, \end{aligned} \tag{9}$$

where $t = [t_X\, t_Y\, t_Z\, 0]$, $q_d = [q_{d_0}\, q_{d_1}\, q_{d_2}\, q_{d_3}]^T$ and $\alpha = [\alpha_0\, \alpha_1\, \alpha_2\, \alpha_3]^T$. The approach proposed in Bektas (2022) determines the scale factor and rotation parameters using the α quaternions while the α and q_d quaternions are used to determine the translation parameters. Hence, the matrix R is determined based on the dual quaternion theory from Equation (10):

$$\begin{aligned} R &= \left(\alpha_0^2 - \alpha^T \times \alpha\right) I_{3\times 3} + 2\left(\alpha \times \alpha^T\right) + \alpha_0 \times C(\alpha), \\ \alpha &= \left[\alpha_1 \alpha_2 \alpha_3\right]^T. \end{aligned} \tag{10}$$

Equation (11) presents the functional model for the 3D transformation in dual quaternion where λ is the scale parameter. Since there are more observations than unknowns, the transformation parameters are determined based on the least squares. However, Equation (11) is non-linear and therefore requires initial approximate values to solve for the unknown transformation parameters. Here, only $\alpha_{0,0}$ is set to 1 and $\alpha_{1,0} = \alpha_{2,0} = \alpha_{3,0} = q_{d_{0,0}} = q_{d_{1,0}} = q_{d_{2,0}} = q_{d_{3,0}} = 0$. A detailed explanation of how the linearization is done is presented in Bektas (2022).

$$\begin{aligned} X_T &= 2W_{(\alpha)}^T \times q_d + \lambda W_{(\alpha)}^T \times Q_{(\alpha)} x_S, \\ \begin{bmatrix} X \\ Y \\ Z \\ 0 \end{bmatrix}_{Pi} &= 2W_{(\alpha)}^T \times q_d + \lambda W_{(\alpha)}^T \times Q_{(\alpha)} \begin{bmatrix} x \\ y \\ z \\ 0 \end{bmatrix}_{Pi}, \end{aligned} \tag{11}$$

where:

$$Q(\alpha) = \begin{bmatrix} \alpha_0 I + C(\alpha) & \alpha \\ -\alpha^T & \alpha_0 \end{bmatrix} = \begin{bmatrix} \alpha_0 & -\alpha_3 & \alpha_2 & \alpha_1 \\ \alpha_3 & \alpha_0 & -\alpha_1 & \alpha_2 \\ -\alpha_2 & \alpha_1 & \alpha_0 & \alpha_3 \\ -\alpha_1 & -\alpha_2 & -\alpha_3 & \alpha_0 \end{bmatrix}, \tag{12}$$

$$W(\alpha) = \begin{bmatrix} \alpha_0 I - C(\alpha) & \alpha \\ -\alpha^T & \alpha_0 \end{bmatrix} = \begin{bmatrix} \alpha_0 & \alpha_3 & -\alpha_2 & \alpha_1 \\ -\alpha_3 & \alpha_0 & \alpha_1 & \alpha_2 \\ \alpha_2 & -\alpha_1 & \alpha_0 & \alpha_3 \\ -\alpha_1 & -\alpha_2 & -\alpha_3 & \alpha_0 \end{bmatrix}, \tag{13}$$

$$\lambda = \alpha_0^2 + \alpha_1^2 + \alpha_2^2 + \alpha_3^2. \tag{14}$$

3.2 Transformation model performance indicators

To ascertain the validity of the transformation results, statistical measures such as root mean square (RMSE), horizontal error (HE), root mean square HE ($\mathrm{RMSE_{HE}}$), standard deviation of HE ($\mathrm{SD_{HE}}$), and maximum and minimum HE were applied. These statistical measures are in line with scholarly practice in coordinate transformation studies (Varga et al., 2017). To carry out the quantitative assessment, the statistical measures (Equations (15–20)) were applied to the estimated error components of the plane coordinates (Easting and Northing).

$$\mathrm{RMSE}_E = \sqrt{\frac{\sum_{i=1}^{n}(E_i - \hat{E}_i)^2}{n}}, \quad \mathrm{RMSE}_N = \sqrt{\frac{\sum_{i=1}^{n}(N_i - \hat{N}_i)^2}{n}}, \tag{15}$$

$$\mathrm{HE} = \sqrt{\left(E_i - \hat{E}_i\right)^2 + \left(N_i - \hat{N}_i\right)^2} = \sqrt{\Delta E^2 + \Delta N^2}, \tag{16}$$

$$\mathrm{RMSE_{HE}} = \sqrt{(\mathrm{RMSE}_E)^2 + (\mathrm{RMSE}_N)^2}, \tag{17}$$

$$\mathrm{SD} = \sqrt{\frac{\sum_{i=1}^{n}\left(\mathrm{HE} - \overline{\mathrm{HE}}\right)^2}{n}}, \tag{18}$$

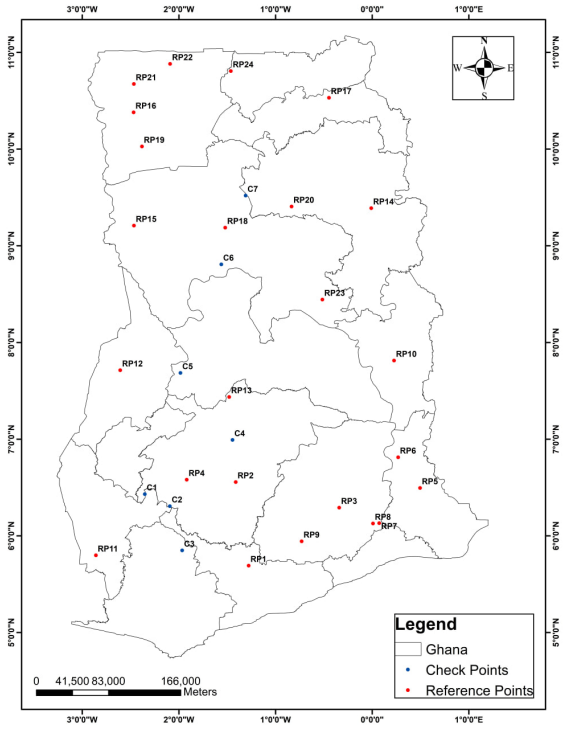

Figure 2. Reference and check points distribution

$$\text{Max} = \text{maximum}(\text{HE}), \tag{19}$$

$$\text{Min} = \text{minimum}(\text{HE}), \tag{20}$$

where (E_i, N_i) and $(\hat{E}_i, \hat{N}_i)$ are the observed and transformed coordinates for Easting and Northing. The RMSE_E and RMSE_N are the RMSE in Easting and Northing, and n is the total observed points.

4 Results and discussion

4.1 Derived dual quaternion transformation parameters for Ghana's geodetic reference network

This study applied a total of 31 common points found in the WGS84 and War Office 1926 for the transformation exercise. Out of the 31 common points, 24 representing 79% served as reference points and were used to derive the transformation parameters. The remaining 7 common points representing 21% were used as check points to evaluate the precision and accuracy of the derived transformation parameters. The distribution of the selected reference and check points is presented in Figure 2. It is important to note that the reference points must be carefully selected. One rule of thumb states that the initial selected reference points must cover the greater extent of the study area. As soon as this is achieved, additional reference points can be added by ensuring that the selected points are distributed evenly across the study area. Hence, in this study, RP11, RP 12, RP15, RP19, RP16, RP21, RP22, RP 24, RP17, RP14, RP10, RP6, RP5, RP7, and RP1 were first selected based on their locations (see Figure 2) because they cover the far extent of the country (Ghana). Additional points (RP2, RP3, RP4, RP8, RP9, RP13, RP18, RP20, and RP23) were then selected and added to the initial reference points by making sure they were homogenously distributed across the country. As seen in Figure 2, the determined transformation parameters will not be extrapolated to produce results since new points to be transformed are found within the reference points utilized to establish those parameters (Bektas, 2022).

Table 2 presents the estimated transformation parameters using the dual quaternion algorithm. The algorithm outputs (Table 2)

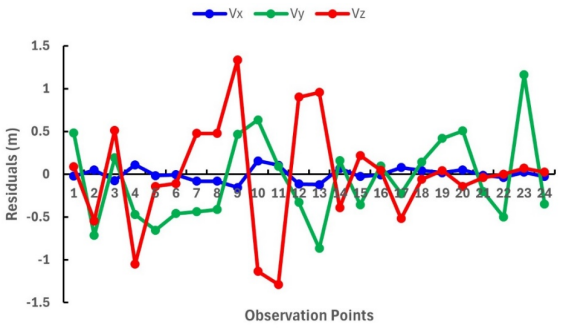

Figure 3. Least squares residual results for 24 control points

include three translation parameters (Tx, Ty, Tz), three rotation parameters (Rx, Ry, Rz), scale factor (L), unit dual quaternion elements ($\alpha 0$, $\alpha 1$, $\alpha 2$, $\alpha 3$, q_{d0}, q_{d1}, q_{d2}, q_{d3}) and the respective precisions (standard deviation) of the parameters.

The least squares residuals (Vx, Vy, Vz) matrix for the (X, Y, Z) cartesian coordinates of the reference points are shown in Table 3. The residual information is further illustrated in Figure 3. In Figure 3, Vx is seen to be very close to the zero residual which was closely followed by Vy and Vz, respectively. The level of heterogeneity in the classical geodetic reference network may have contributed to the departing extent and the level of volatility experienced with the residuals from the ideal zero value.

4.2 Dual quaternion transformation results

To assess the performance of the dual quaternion algorithm, the derived transformation parameters were applied to transform the WGS84 coordinates into the War Office 1926 system. This transformation was made because the War Office 1926 is the official mapping reference for survey activities in Ghana. Tables 4 and 5 present the coordinate differences for the reference and check points between the transformed cartesian (X, Y, Z) coordinates and the measured points in War Office 1929.

Since the projected grid coordinates are used for all surveying and mapping activities in Ghana, map projection was conducted on the transformed coordinates. Tables 6 and 7 present the resultant differences between the transformed and measured grid coordinates for 24 reference and 7 check points. At a glance, it is noted in Table 6 that the reference points RP4, RP9, RP10, and RP12 had a discrepancy above 1 metre in the Northing component with the Easting having a discrepancy below 1 metre. Similar differences above 1 metre were also associated with the check points for the Easting (C2) and Northing (C1, C3, and C5) components (Table 7). The size of the error may be due to possible distortions that are usually associated with classical geodetic networks due to how it was established. For instance, the Ghana geodetic network was established based on two separate surveys where triangulation was used to fix the controls in the Southing part of the country and traversing was used in the Northing part. Historical accounts also indicate that the triangulation and traverse surveys were adjusted separately (Poku-Gyamfi, 2009). Hence, the discrepancy observed could be the consequence of how the classical geodetic network was established and adjusted in Ghana.

To provide a comprehensive assessment of the results presented in Tables 6 and 7, summary statistics of the discrepancies for both reference and check points are presented in Table 8. It can be inferred from the error estimations (Table 8) that the distortion ranges of the reference points were 0.1112–1.4173 m, and the check points were 0.1351–1.4971 m in the minimum and maximum. This implies that in the worst-case scenario, the determined transformation parameters can transform a single point that would not deviate more than 1.4971 m from its measured coordinate. Similarly, it can

Table 2. Computed dual quaternion algorithm transformation parameters

Parameter	Value	Unit	Description
Tx	143.68728309±4.392876233211001	m	Translation in X
Ty	-30.97180602±9.090202365889539	m	Translation in Y
Tz	-329.27294604±5.378363851725634	m	Translation in Z
Rx	0.0004235948034±0.000000711958960	degree	Rotation in X
Ry	-0.0000034240300±0.000000845173900	degree	Rotation in Y
Rz	0.0000602917607±0.000001413450798	degree	Rotation in Z
L	1.000008301±0.000000685997524	-	Scale Factor
$\alpha 0$	0.999999999993	-	Unit Dual Quaternion Elements
$\alpha 1$	-0.000003696562	-	
$\alpha 2$	0.000000029882	-	
$\alpha 3$	-0.000000526145	-	
q_{d0}	71.843654612490	-	
q_{d1}	-15.485256620946	-	
q_{d2}	-164.636528118377	-	
q_{d3}	0.000179414611	-	

Table 3. Least squares residual matrix for the reference point (RP) used to derive the transformation parameters

Point ID	Vx (m)	Vy (m)	Vz (m)
RP1	-0.0224	0.4818	0.0879
RP2	0.0498	-0.7145	-0.5457
RP3	-0.0749	0.1912	0.5122
RP4	0.1107	-0.4722	-1.0477
RP5	-0.0150	-0.6546	-0.1410
RP6	-0.0048	-0.4587	-0.1082
RP7	-0.0811	-0.4372	0.4768
RP8	-0.0803	-0.4122	0.4779
RP9	-0.1545	0.4656	1.3331
RP10	0.1553	0.6348	-1.1342
RP11	0.1053	0.0930	-1.2870
RP12	-0.1152	-0.3294	0.9022
RP13	-0.1213	-0.8655	0.9559
RP14	0.0677	0.1590	-0.3894
RP15	-0.0274	-0.3564	0.2187
RP16	-0.0077	0.0951	0.0462
RP17	0.0782	-0.2260	-0.5181
RP18	0.0428	0.1422	-0.0591
RP19	0.0177	0.4194	0.0437
RP20	0.0512	0.5075	-0.1426
RP21	-0.0145	-0.2026	-0.0383
RP22	-0.0364	-0.5008	0.0018
RP23	0.0233	1.1606	0.0700
RP24	-0.0269	-0.3486	0.0240

Table 4. Error margin between the transformed and measured War Office 1929 coordinates for the reference point (RP) (unit: metres)

Point ID	ΔX	ΔY	ΔZ
RP1	-0.0223	0.4817	0.0879
RP2	0.0498	-0.7145	-0.5457
RP3	-0.0750	0.1912	0.5122
RP4	0.1107	-0.4722	-1.0477
RP5	-0.0150	-0.6546	-0.1410
RP6	-0.0048	-0.4588	-0.1082
RP7	-0.0811	-0.4372	0.4768
RP8	-0.0803	-0.4122	0.4779
RP9	-0.1546	0.4656	1.3331
RP10	0.1553	0.6347	-1.1342
RP11	0.1053	0.0930	-1.2870
RP12	-0.1153	-0.3294	0.9022
RP13	-0.1214	-0.8655	0.9560
RP14	0.0678	0.1590	-0.3895
RP15	-0.0274	-0.3564	0.2187
RP16	-0.0077	0.0952	0.0462
RP17	0.0781	-0.2261	-0.5181
RP18	0.0428	0.1422	-0.0591
RP19	0.0176	0.4194	0.0438
RP20	0.0512	0.5075	-0.1426
RP21	-0.0145	-0.2026	-0.0383
RP22	-0.0364	-0.5008	0.0018
RP23	0.0233	1.1606	0.0701
RP24	-0.0270	-0.3486	0.0240
Maximum	0.1553	1.1606	1.3331
Minimum	-0.1546	-0.8655	-1.2870
SD	0.0867	0.5636	0.7081

Table 5. Error margin between transformed WGS84 and existing War Office 1929 for the check points (C) (unit: metres)

Point ID	ΔX	ΔY	ΔZ
C1	0.0896	-0.2755	-1.1477
C2	-0.0502	-1.4575	-0.1055
C3	0.1040	-0.4012	-1.1086
C4	-0.0017	0.0772	0.1511
C5	-0.1748	-0.5909	1.3435
C6	-0.0089	-0.3198	0.2146
C7	0.0410	0.3191	-0.0610
Maximum	0.1040	0.3191	1.3435
Minimum	-0.1748	-1.4575	-1.1477
SD	0.0946	0.5654	0.8527

Table 6. Differences in projected grid coordinates based on the reference points (unit: metres)

Point ID	ΔN	ΔE	HE
RP1	0.0885	0.4810	0.4890
RP2	-0.5541	-0.7133	0.9033
RP3	0.5160	0.1742	0.5446
RP4	-1.0560	-0.4796	1.1598
RP5	-0.1066	-0.6164	0.6256
RP6	-0.0686	-0.4915	0.4962
RP7	0.4886	-0.4270	0.6489
RP8	0.4857	-0.4170	0.6401
RP9	1.3410	0.4588	1.4173
RP10	-1.1155	0.6187	1.2756
RP11	-0.9615	0.0703	0.9640
RP12	1.0375	-0.3445	1.0932
RP13	0.9561	-0.8676	1.2911
RP14	-0.3995	0.1595	0.4302
RP15	0.2299	-0.3567	0.4244
RP16	0.0578	0.0950	0.1112
RP17	-0.5331	-0.2249	0.5786
RP18	-0.0727	0.1430	0.1604
RP19	0.0475	0.4190	0.4217
RP20	-0.1557	0.5082	0.5315
RP21	-0.0242	-0.2032	0.2047
RP22	0.0042	-0.5023	0.5023
RP23	0.0625	1.1605	1.1622
RP24	0.0178	-0.3490	0.3495

Table 7. Differences in projected grid coordinates based on the reference points (unit: metres)

Point ID	ΔN	ΔE	HE
C1	-1.1479	-0.2601	1.1770
C2	-0.0634	-1.4498	1.4512
C3	-1.1140	-0.4135	1.1882
C4	0.1207	0.0608	0.1351
C5	1.3434	-0.6608	1.4971
C6	0.2058	-0.3197	0.3802
C7	-0.0740	0.3198	0.3282

Table 8. Summary statistics of the transformation results for both reference and check points (unit: metres)

Statistical Indicator	Reference Point	Check Point
RMSE East	0.4948	0.6531
RMSE North	0.6014	0.7955
RMSE HE	0.7788	1.0292
Average HE	0.6844	0.8796
Maximum HE	1.4173	1.4971
Minimum HE	0.1112	0.1351
SD	0.3797	0.5773

transform a single point that would deviate from the measured coordinate only by 0.1351 m in the classical geodetic network of Ghana. Averagely, the horizontal positional accuracy between the transformed and measured coordinates varies between 0.6844–0.8796 m when one considers the reference and check points. In the Easting and Northing components, the RMSE values indicate achieved reasonable degree of dispersion between transformed and measured coordinates. Based on the RMSE HE results, it can be stated that a transformation accuracy between 0.7788–1.0292 m can be achieved in unifying the WGS84 and War Office 1929 systems. Considering the reference and check points, it is observed that a transformation precision ranging from 0.3797–0.5773 m is attainable.

4.3 Comparing dual quaternion algorithm and Bursa-Wolf model

In Ghana, the Bursa-Wolf transformation model is the most widely accepted coordinate approach to perform 3D coordinate transformation. It is also the technique used to determine the official transformation parameters utilized in the country. Considering this, it is prudent to make a comparison between the proposed dual quaternion algorithm and the Bursa-Wolf transformation model. This comparison was to confirm the reliability of the dual quaternion as an alternative transformation approach to the Bursa-Wolf model. The estimated parameters and standard deviation of the Bursa-Wolf model are listed in Table 9. The computed horizontal residuals for the reference and check points showed identical results (Figs. 4 and 5). The same summary statistics (Table 10) were obtained in all methods. Thus, no significant difference exists between the different transformation method solutions. Accordingly, the proposed dual quaternion algorithm is valid for 3D coordinate transformation in Ghana.

These results (Table 10) prove that both methods achieved a meter-level transformation accuracy, which meets the demands of some surveying and mapping activities in Ghana such as cadastral surveying, geographic information works, reconnaissance, land information system works, and small-scale topographic surveys (Yakubu and Kumi-Boateng, 2015). Although the methods achieved a meter-level accuracy, cognitive analysis of the results indicates that the derived parameters can also produce a centimetre-level accuracy when transforming new coordinates. This can be seen from the reported minimum HE produced by both methods. Therefore, the inference here is that the estimated transformation parameters between WGS84 and War Office 1929 are restricted to the region where the common points are located.

4.4 Limitations of the study

The dual quaternion algorithm and Bursa-Wolf model in its original formulation do not consider the distortions that are exhibited by coordinates that are related to the classical geodetic network. Hence, the transformation results achieved in this study are valid only for its intended purposes. However, for high-precision sur-

Table 9. Computed Bursa-Wolf transformation parameters

Parameter	Value	Unit
Tx	-144.404369432623±2.71644169249343	m
Ty	30.8392251366517±5.77913539479517	m
Tz	328.969752734147±3.31299131230516	m
Rx	$-1.54225613813615 \pm 4.41022399239605 \times 10^{-07}$	rad
Ry	$0.0194187287742367 \pm 5.20304861273006 \times 10^{-07}$	rad
Rz	$-0.226456753173654 \pm 8.98852336716549 \times 10^{-07}$	rad
S	$-8.182912801433343 \pm 4.24566775106515 \times 10^{-07}$	ppm

Table 10. Summary statistics of the horizontal residuals for both methods (unit: metres)

Statistical Indicator	Bursa-Wolf		Dual Quaternion	
	Reference Point	Check Point	Reference Point	Check Point
RMSE East	0.4948	0.6531	0.4948	0.6531
RMSE North	0.6014	0.7955	0.6014	0.7955
SD	0.3797	0.5773	0.3797	0.5773
RMSE HE	0.7788	1.0292	0.7788	1.0292
Maximum HE	1.4173	1.4971	1.4173	1.4971
Minimum HE	0.1112	0.1351	0.1112	0.1351

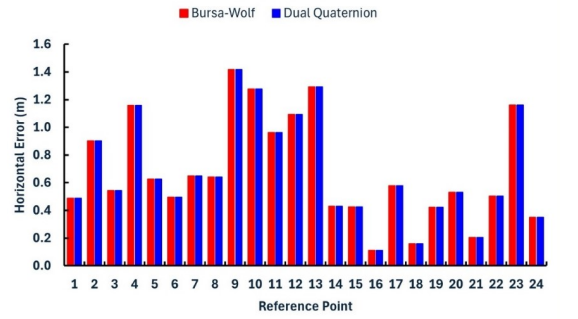

Figure 4. Reference points horizontal residuals

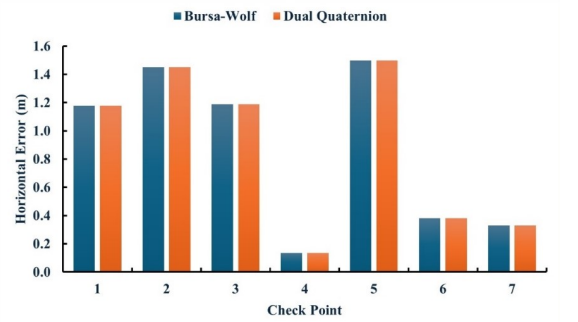

Figure 5. Check points horizontal residuals

veys, it is recommended that the distortion must be considered during the transformation parameters derivation. This is in line with the assertion made by Shen et al. (2006) that the distortions are integrated into the derived transformation parameters if not adequately handled during the transformation process.

5 Conclusions

In the current conditions of most Sub-Saharan African countries such as Ghana, the geodetic infrastructure lacks geocentric datum as its official mapping reference system. This makes the determination of parameters for coordinate transformation relevant. Therefore, it is justified to assess the capability of other transformation techniques. The dual quaternion algorithm was applied and evaluated to transform coordinates between WGS84 and Ghana War Office 1929 classical geodetic system. The results revealed a transformation accuracy and precision ranging from 0.7788–1.0292 m and 0.3797–0.5773 m for the reference and check points. These results confirmed that the transformed coordinates by the dual quaternion algorithm are in average agreement with the measured coordinates at the level of about 0.5773 m. Similar residual differences were obtained when the dual quaternion was compared with the Bursa-Wolf model, with the former confirming its suitability to serve as an alternative transformation technique in Ghana. To improve the statistical residual differences obtained between the transformed and measured coordinates, the systematic distortions in the data related to the local datum must be considered in the transformation process.

References

Ansari, K., Corumluoglu, O., and Yetkin, M. (2017). Projectivity, affine, similarity and euclidean coordinates transformation parameters from ITRF to EUREF in Turkey. *Journal of Applied Geodesy*, 11(1):53–61, doi:10.1515/jag-2016-0040.

Ansari, K., Gyawali, P., Pradhan, P. M., and Park, K.-D. (2019). Coordinate transformation parameters in Nepal by using neural network and SVD methods. *Journal of Geodetic Science*, 9(1):22–28, doi:10.1515/jogs-2019-0003.

Bektas, S. (2022). A new algorithm for 3D similarity transformation with dual quaternion. *Arabian Journal of Geosciences*, 15(14):1273, doi:10.1007/s12517-022-10457-z.

Bektas, S. (2024). An expanded dual quaternion algorithm for 3D Helmert transformation and determination of the VCV matrix of the transformation's parameters. *Journal of Spatial Science*, 69(2):665–680, doi:10.1080/14498596.2023.2274997.

Doukas, I. D., Ampatzidis, D., and Kampouris, V. (2017). The validation of the transformation between an old geodetic reference frame and a modern reference frame, by using external space techniques sites: The case study of the hellenic geodetic reference system of 1987. *Boletim de Ciências Geodésicas*, 23(3):434–444, doi:10.1590/S1982-21702017000300029.

Elshambaky, H., Kaloop, M. R., and Hu, J. W. (2018). A novel three-direction datum transformation of geodetic coordinates for Egypt using artificial neural network approach. *Arabian Journal of Geosciences*, 11:1–14, doi:10.1007/s12517-018-3441-6.

Hussain, R. Y. (2022). Coordinate transformation from Karbala 1979 and World Geodetic System 1984 to Iraqi Geospatial Reference System. *Journal of Engineering and Sustainable Development*, 26(3):73–83, doi:10.31272/jeasd.26.3.8.

Ioannidou, S. and Pantazis, G. (2020). Helmert transformation problem. From Euler angles method to quaternion algebra. *ISPRS International Journal of Geo-Information*, 9(9):494, doi:10.3390/ijgi9090494.

Ioannidou, S. and Pantazis, G. (2022). *3D Coordinate Transformation by using Quaternion Algebra*, page 1–24. Book Publisher International, doi:10.9734/bpi/tier/v5/16305d.

Kalu, I., Ndehedehe, C. E., Okwuashi, O., and Eyoh, A. E. (2022). Estimating the seven transformational parameters between two geodetic datums using the steepest descent algorithm of machine learning. *Applied Computing and Geosciences*, 14:100086, doi:10.1016/j.acags.2022.100086.

Kenwright, B. (2012). A beginners guide to dual-quaternions: What they are, how they work, and how to use them for 3D character hierarchies. In *20th International Conference in Central Europe on Computer Graphics, Visualization and Computer Vision 2012, Plzen, Czech Republic, June 26–28*, pages 1–10.

Kheloufi, N. and Dehni, A. (2023). Some mathematical assumptions for accurate transformation parameters between WGS84 and Nord Sahara geodetic systems. *Journal of Geodetic Science*, 13(1):20220160, doi:10.1515/jogs-2022-0160.

Mercan, H., Akyilmaz, O., and Aydin, C. (2018). Solution of the weighted symmetric similarity transformations based on quaternions. *Journal of geodesy*, 92(10):1113–1130, doi:10.1007/s00190-017-1104-0.

Mihajlović, D. and Cvijetinović, Ž. (2017). Weighted coordinate transformation formulated by standard least-squares theory. *Survey review*, 49(356):328–345, doi:10.1080/00396265.2016.1173329.

Okiemute, E. S., Oduyebo, O. F., and Olulade, S. A. (2018). Comparative analysis of three geodetic datum transformation software for application between WGS84 and Minna datums. *International Journal of Engineering Science and Computing*, 8(12):19410–19417.

Poku-Gyamfi, Y. (2009). *Establishment of GPS reference network in Ghana*. PhD thesis, Universitat der Bundeswehr Munchen, Germany.

Prasad, K. and Prasanna, H. (2022). Determination of 3D transformation parameters for the Sri Lankan Geodetic Reference Network using ordinary and total least squares. *Journal of Geospatial Surveying*, 2(2):11–21, doi:10.4038/jgs.v2i2.39.

Ruffhead, A. (2021). Derivation of rigorously-conformal 7-parameter 3D geodetic datum transformations. *Survey Review*, 53(376):8–15, doi:10.1080/00396265.2019.1665614.

Shen, Y. Z., Chen, Y., and Zheng, D. H. (2006). A quaternion-based geodetic datum transformation algorithm. *Journal of Geodesy*, 80:233–239, doi:10.1007/s00190-006-0054-8.

Soler, T., Han, J.-Y., and Weston, N. D. (2016). Variance-covariance matrix of transformed GPS positions: Case study for the NAD 83 geodetic datum. *Journal of Surveying Engineering*, 142(1):04015004, doi:10.1061/(ASCE)SU.1943-5428.0000143.

Uygur, S. Ö., Akyilmaz, O., and Aydin, C. (2021). Solution of nine-parameter affine transformation based on quaternions. *Journal of Surveying Engineering*, 147(3):04021011, doi:10.1061/(ASCE)SU.1943-5428.0000364.

Uygur, S. Ö., Aydin, C., and Akyilmaz, O. (2022). Retrieval of Euler rotation angles from 3D similarity transformation based on quaternions. *Journal of Spatial Science*, 67(2):255–272, doi:10.1080/14498596.2020.1776170.

Varga, M., Grgić, M., and Bašić, T. (2017). Empirical comparison of the Geodetic Coordinate Transformation Models: A case study of Croatia. *Survey Review*, 49(352):15–27, doi:10.1080/00396265.2015.1104092.

Wang, Y., Wang, Y., Wu, K., Yang, H., and Zhang, H. (2014). A dual quaternion-based, closed-form pairwise registration algorithm for point clouds. *ISPRS journal of photogrammetry and remote sensing*, 94:63–69, doi:10.1016/j.isprsjprs.2014.04.013.

Yakubu, I. and Kumi-Boateng, B. (2015). Ramification of datum and ellipsoidal parameters on post processed differential global positioning system (DGPS) data – A case study. *Ghana Mining Journal*, 15(1):1–9.

Zeng, H., Chang, G., He, H., and Li, K. (2020). WTLS iterative algorithm of 3D similarity coordinate transformation based on Gibbs vectors. *Earth, Planets and Space*, 72:1–12, doi:10.1186/s40623-020-01179-1.

Zeng, H., Chang, G., He, H., Tu, Y., Sun, S., and Wu, Y. (2019). Iterative solution of Helmert transformation based on a unit dual quaternion. *Acta geodaetica et geophysica*, 54:123–141, doi:10.1007/s40328-018-0241-0.

Zeng, H., Fang, X., Chang, G., and Yang, R. (2018). A dual quaternion algorithm of the Helmert transformation problem. *Earth, Planets and Space*, 70:1–12, doi:10.1186/s40623-018-0792-x.

Zeng, H., He, H., Chen, L., Chang, G., and He, H. (2022a). Extended WTLS iterative algorithm of 3D similarity transformation based on Gibbs vector. *Acta Geodaetica et Geophysica*, pages 1–19, doi:10.1007/s40328-021-00363-3.

Zeng, H., Wang, J., Wang, Z., Li, S., He, H., Chang, G., and Yang, R. (2022b). Analytical dual quaternion algorithm of the weighted three-dimensional coordinate transformation. *Earth, Planets and Space*, 74(1):170, doi:10.1186/s40623-022-01731-1.

Zeng, H., Wang, Z., Li, J., Li, S., Wang, J., and Li, X. (2024). Dual-quaternion-based iterative algorithm of the three dimensional coordinate transformation. *Earth, Planets and Space*, 76(1):20, doi:10.1186/s40623-024-01967-z.

Zhao, Z., Li, Z., and Wang, B. (2024). A novel robust quaternions-based algorithm for 3-D symmetric similarity datum transformation. *IEEE Transactions on Instrumentation and Measurement*, 73(1003012):1–12, doi:10.1109/TIM.2024.3370773.